



UNIVERSITY OF LEEDS

This is a repository copy of *Transient Analysis of THz-QCL Pulses Using NbN and YBCO Superconducting Detectors*.

White Rose Research Online URL for this paper:
<http://eprints.whiterose.ac.uk/75245/>

Article:

Scheuring, A, Dean, P, Valavanis, A et al. (12 more authors) (2013) Transient Analysis of THz-QCL Pulses Using NbN and YBCO Superconducting Detectors. *IEEE Transactions on Terahertz Science and Technology*, 3 (2). pp. 172-179. ISSN 2156-342X

<https://doi.org/10.1109/TTHZ.2012.2228368>

Reuse

Unless indicated otherwise, fulltext items are protected by copyright with all rights reserved. The copyright exception in section 29 of the Copyright, Designs and Patents Act 1988 allows the making of a single copy solely for the purpose of non-commercial research or private study within the limits of fair dealing. The publisher or other rights-holder may allow further reproduction and re-use of this version - refer to the White Rose Research Online record for this item. Where records identify the publisher as the copyright holder, users can verify any specific terms of use on the publisher's website.

Takedown

If you consider content in White Rose Research Online to be in breach of UK law, please notify us by emailing eprints@whiterose.ac.uk including the URL of the record and the reason for the withdrawal request.



eprints@whiterose.ac.uk
<https://eprints.whiterose.ac.uk/>

Transient analysis of THz-QCL pulses using NbN and YBCO superconducting detectors

Alexander Scheuring, Paul Dean, Alex Valavanis, Axel Stockhausen, Petra Thoma, Mohammed Salih, Suraj P. Khanna, Siddhant Chowdhury, Jonathan D. Cooper, Andrew Grier, Stefan Wuensch, Member, IEEE, Konstantin Il'in, Edmund H. Linfield, A. Giles Davies and Michael Siegel

Abstract—We report the time-domain analysis of fast pulses emitted by a quantum cascade laser (QCL) operating at ~ 3.1 THz using superconducting THz detectors made from either NbN or $\text{YBa}_2\text{Cu}_3\text{O}_{7.8}$ (YBCO) thin films. The ultra-fast response from these detectors allows resolution of emission features occurring on a nanosecond time-scale, which is not possible with commercially available Ge or InSb bolometers owing to their much larger time constants. We demonstrate that the time-dependent emission can be strongly affected by relatively small variations in the driving pulse. The QCL output power–current relationship was determined, based on correlation of the time-dependent emission of radiation with current flow in the QCL, under different QCL bias conditions. We show that this relationship differs from that obtained using bolometric detectors that respond only to the integrated pulse energy. The linearity of the detectors, and their agreement with measurements using a Ge bolometer, was also established by studying the QCL emission as a function of bias voltage and excitation pulse length. This measurement scheme could be readily applied to the study of ultra-fast modulation and mode-locking of THz-QCLs.

Index Terms— Quantum cascade lasers, Superconducting THz detectors, Pulse measurements, Submillimeter wave measurements.

I. INTRODUCTION

TERAHERTZ frequency quantum cascade lasers (THz-QCLs) are powerful, yet compact, solid-state sources of coherent THz radiation over the frequency range 1.2 to 5 THz [1]–[3]. The high output power (exceeding 250 mW in pulsed operation [4]), narrow linewidths (<30 kHz [5]) and broad range of achievable emission frequencies give rise to numerous potential applications [6], including imaging [7], [8] and spectroscopy [9], as well as their use as local oscillators in

heterodyne mixing schemes [10].

A wide range of techniques has been previously employed for the detection of THz-QCL radiation. A number of these are sensitive to the THz electric field, making coherent sampling possible. These include mixing in Schottky diodes [11], GaAs photomixers [12], and hot-electron bolometers [13], as well as ultra-fast electro-optic sampling [14]. Nevertheless, the most common THz direct detection technologies such as room-temperature pyroelectric sensors, Golay cells and cryogenically-cooled semiconducting bolometers, rely on incoherent thermal detection of radiation. Owing to the slow time-constants of thermal processes (typically ~ 0.1 –10 ms), such schemes are sensitive only to the total pulse energy for typical pulsed QCL operating conditions. The QCL characteristics measured in this manner do not, therefore, provide a true representation of the current–power relationship of the laser since driving pulses typically exhibit some dynamic variation in amplitude. The slow response also precludes the investigation of intra-pulse dynamics, which can occur on fast time-scales owing to the lifetime of the upper state of the lasing transition being limited to a few picoseconds by elastic and inelastic scattering mechanisms in THz-QCLs [15]. Whilst fast transient phenomena have been observed using ultra-fast electro-optic sampling techniques [14], this approach is complex and costly and data acquisition is relatively slow. Schottky diode detectors also exhibit a short response time (in the picosecond range). However, for these diode detectors a noise equivalent power (NEP) in the range of 10^{-11} – 10^{-10} W/ $\sqrt{\text{Hz}}$ has been reported [16], [17], which is more than one order of magnitude above the detection limit of superconducting detectors [18], [19]. Moreover, Schottky diodes show a nonlinear detector response [16].

In this paper, we report on the time-domain analysis of fast QCL pulses using superconducting direct detectors made from either NbN or $\text{YBa}_2\text{Cu}_3\text{O}_{7.8}$ (YBCO) thin films. The ultra-fast detector response allows laser emission features to be resolved on a nanosecond time-scale. The QCL output power–current relationship is determined based on a correlation between the measured time-dependent emission of radiation with current flow, enabling the interpretation of the time-domain detector responses to QCL pulses of varying amplitude and duration. This work demonstrates the applicability of superconducting direct detectors to ultra-fast analysis of QCL emission. This scheme could also readily be applied to the study of ultra-fast

Manuscript received August 27, 2012. This work was partly supported by the German Federal Ministry of Education and Research (Grant No. 05K2010 and Grant No. 13N12025) and by DFG Center for Functional Nanostructures. We also acknowledge funding from the UK Engineering and Physical Sciences Research Council, the European Research Council grants ‘TOSCA’ and ‘NOTES’, the Royal Society and the Wolfson Foundation.

A. Scheuring, A. Stockhausen, P. Thoma, S. Wuensch, K. Il'in and M. Siegel are with the Institute of Micro- and Nanoelectronic Systems (IMS) at the Karlsruhe Institute of Technology (KIT), 76187 Karlsruhe, Germany (corresponding author email: a.scheuring@kit.edu).

P. Dean, A. Valavanis, M. Salih, S. P. Khanna, S. Chowdhury, J. D. Cooper, A. Grier, E. H. Linfield and A. G. Davies are with the School of Electronic and Electrical Engineering, University of Leeds, Leeds LS2 9JT, UK.

modulation of THz-QCLs [20] as well as the study of mode-locking [14] of THz-QCLs, for which fast detection is required to resolve the mode-locked pulses that occur at the typically <100 ps round-trip time of the laser cavity.

II. EXPERIMENTAL SETUP

The QCL used for this work was based on a three-well resonant-phonon depopulation scheme emitting at ~ 3.1 THz [21]. THz-QCLs based on this scheme typically suffer from the presence of strong parasitic current channels that artificially enhance the threshold current [22], [23]. In addition, owing to the requirement to drop >36 meV (the LO phonon energy in GaAs) across each individual module of this structure, large applied biases are required at threshold. Both of these factors lead to large electrical power dissipation in such QCLs, making continuous wave operation challenging. Consequently, such QCLs are invariably operated in pulsed mode, for which determination of the correct current–power relationship of the laser is challenging, as previously noted. The device was processed into a semi-insulating surface plasmon ridge waveguide with dimensions $0.85 \text{ mm} \times 140 \text{ }\mu\text{m} \times 10 \text{ }\mu\text{m}$. Fig. 1 shows a schematic of the experimental apparatus. The QCL was operated in a continuous flow liquid-helium-cooled cryostat at a constant temperature of 15 K. The laser was driven by a pulse generator (Agilent 8114A) at a repetition rate of $f_{\text{rep}}=10$ kHz, with either the amplitude or length of the driving pulses being varied. The time-dependent current flow through the QCL was monitored using an inductive current probe with a minimum measurable pulse duration of 5 ns. The emitted THz radiation was focused by two off-axis parabolic mirrors onto the detector block, which was mounted in a separate optical cryostat. For the experiment the use of a separate cryostat allows the flexible adjustment of temperature to achieve optimum operating conditions of the detectors. Nevertheless, it is also possible to integrate both QCL and detector into a single cooling system as it has been demonstrated for heterodyne receiver applications [24]. The detector elements consisted of NbN or YBCO micro-bridges fabricated on a sapphire substrate (thickness=330 μm , $\epsilon_r=10.06$). The detectors were operated at a temperature T_{op} below their critical temperature T_c and driven onto the superconducting transition by a constant bias voltage. The geometry and operating conditions for both detector types are listed in Table I. Further details about the detector fabrication can be found in [25] for the NbN and [26] for the YBCO technologies. Owing to the sub-wavelength geometry, the detector bridges were embedded into a planar log-spiral antenna, made from 200-nm-thick gold, to improve the input radiation coupling efficiency. The spiral antenna was designed to cover a broad frequency range from 0.5–4 THz. For the high-frequency readout, the antenna was connected to a coplanar waveguide, and the $3 \times 3 \text{ mm}^2$ detector chip was mounted on the rear side of a 12-mm-diameter silicon lens ($\epsilon_r=11.7$) to focus the incident THz radiation. Further information about the detector block with the integrated

dielectric lens are presented in [27]. Typical intrinsic NbN detector response times are $\tau \approx 30$ ps [28], [29]. For YBCO response times as short as single picoseconds were achieved [30], [31]. These detectors are much faster than commercial Ge or InSb bolometers that exhibit time constants in the microsecond or even millisecond range [32].

The ultra-fast response of superconducting detectors allows resolution of dynamic QCL emission features that occur on a nanosecond time-scale. The detector signal was amplified by a room temperature preamplifier with a bandwidth of 0.1–400 MHz and a signal gain of 40 dB. The amplified signal was monitored using a 500 MHz real-time oscilloscope. According to [33], the effective readout bandwidth f_{eff} is calculated as

$$f_{\text{eff}} = \left[\sum_i f_i^{-2} \right]^{-1/2} = 312.4 \text{ MHz}, \quad (1)$$

where f_i is the bandwidth of the i -th component within the readout chain. The effective readout bandwidth corresponds to a time resolution

$$\tau = \frac{0.35}{f_{\text{eff}}} = 1.1 \text{ ns}. \quad (2)$$

III. MEASUREMENT RESULTS AND ANALYSIS

A. Measurement and analysis of QCL emission dependent on bias voltage

Detector signals were analyzed for QCL bias voltages over the full operating range of the QCL. Fig. 2a shows the time-dependent current flow for different values of the QCL bias voltage U_b , for a pulse length of 500 ns. It should be noted that U_b refers to the bias setting on the pulse generator, although the actual bias supplied to the QCL varies through the duration of the pulse. The approximately-rectangular voltage pulses give rise to similarly-shaped current pulses, although the impedance mismatch produces transient peaks on the rising and falling edges, and on the front part of the current plateau. In the later part of the pulse, the current is quite homogeneous, with a slight increase until the pulse is switched off. As the value of the bias voltage U_b is increased, the different curves show an increase in the QCL current but maintain the same general pulse shape. The detector signals depend linearly on the coupled radiation power due to the wide dynamic range of these detectors (see later and [26], [34]). In contrast to the QCL current, the measured detector signals show a strong variation in both the amplitude and shape of the pulses, as shown in Fig. 2b.

A QCL emits radiation when its drive current exceeds the threshold level determined by the waveguide and mirror losses, the overlap of the waveguide mode with the active region, and the laser gain coefficient. For the analyzed laser, the threshold current ($I_{\text{th}}=1.13$ A) is indicated by the dashed horizontal line in Fig. 2a. For higher bias voltages U_b the drive current reaches the threshold earlier than for lower biases, and therefore the QCL starts emitting radiation earlier after the start of the current pulse. Using our fast superconducting detectors it is possible to resolve such features. This can be seen by comparing the $U_b=14.1$ V and the $U_b=12.6$ V traces in Fig. 2. The first peak of the detector signal appears about 14 ns earlier for the 14.1 V trace (the corresponding peak

being labeled 'I' in Fig. 2b) than for the 12.6 V trace (Fig. 2b-II) because the corresponding current traces reach the threshold level at different points in time (Fig. 2a-I and -II) as a consequence of the specific transient features in these current pulses.

However, a number of additional transient emission features are observed at times when the measured current appears to be below the threshold. For example, the measured detector signal for $U_b=14.1$ V shows an additional pre-pulse (Fig. 2b-III) that appears before the main peak, although the corresponding small spike in the measured current appears to be below the threshold level (Fig. 2a-III). This is attributed to the fact that the bandwidth of the current probe is insufficient to measure the magnitude of this fast transient current peak accurately. The absence of such a pre-pulse in the other detector responses shown in Fig. 2b indicates that the corresponding current peaks do not reach threshold in these cases.

The transfer function relating detector voltage and QCL drive current was derived by direct mapping of the detector signals to the time-equivalent current values within each pulse. To avoid the underestimation of transient currents (as described above), we have restricted the temporal range of our analysis to include only the region of slowly varying current within each pulse (indicated by the dashed vertical lines in Fig. 2a). In this way, it was possible to analyze currents from 1.05–1.52 A obtained from 26 different QCL bias settings U_b . For noise reduction, a robust smoothing filter algorithm was applied to the raw data [35]. The final results for both NbN and YBCO detector measurements are shown in Fig. 3, with each curve normalized to its respective maximum. Due to the good agreement between the results of two different detector types and the fact that both detectors show a linear response with coupled THz power (see later) we conclude that these transfer functions represent the true power–current relationship of the QCL. We can therefore deduce that the laser threshold current is $I_{th}=1.13$ A. Below this level, no radiation is detected. Similarly, above the cut-off level of $I_{cut}=1.36$ A, no radiation is detected. Between these two extremes, there are two emission maxima at around $I=1.20$ A and $I=1.28$ A. It should be noted that the measured power–current relationship shown in Fig. 3 is an inherent characteristic of the QCL device and would in principle be equally applicable to alternative driving conditions, including continuous-wave (c.w.) operation.

Fig. 3 also shows the approximate power–current relationship of the QCL obtained using a helium-cooled germanium (Ge) bolometer. As previously noted, this slow thermal detector measures the integrated pulse energy rather than the instantaneous power–current relationship; the current values measured at the end of the pulse plateau (see Fig. 2a) have been plotted as the abscissa for this curve in Fig. 3. There is a notable discrepancy observed between the ultra-fast traces and the Ge bolometer trace, which is a direct consequence of this slow integral response. It is notable that the Ge bolometer measurement is shifted towards higher current values and also indicates lasing over a larger range of currents than the NbN and YBCO measurements. However, this is an artifact arising from transients in the current pulses, which can cause the QCL to lase instantaneously even when the current at the end of the

plateau is below threshold or above the cut-off level. In order to determine the threshold current accurately from such integral measurements, it is necessary to measure the intra-pulse peak current value at the onset of lasing. This is shown in the inset of Fig. 3, which indicates a threshold current of 1.13 A, in perfect agreement with that obtained from both NbN and YBCO measurements. Further validation of this agreement, with respect to threshold current, has been obtained by comparing the time-integrated response of the superconducting detectors with that of the Ge bolometer.

Of particular noteworthiness is the presence of two local maxima observed in the power-current relationships obtained using the ultra-fast detectors, at currents of approximately $I=1.20$ A and $I=1.28$ A, corresponding to applied voltages of 13.7 V and 14.1 V. These features are not resolved fully using the Ge bolometer. To gain insight into the origin of these features, the QCL active region gain was simulated over a range of applied electric fields, using a semiclassical rate-equations approach. Our simulation method has been described in detail previously [36], and may be summarized as follows. Firstly, the potential profile in the direction of material growth was estimated by adding a one-dimensional solution of the Poisson equation to the conduction band profile. Initially, a uniform spatial distribution of free electrons was assumed. The corresponding quasibound eigenstates of the system were then found by solving the one-dimensional Schrödinger equation, accounting for band nonparabolicity, as described in [37].

The population of each electronic subband was computed by solving a system of rate-equations, accounting for intersubband scattering due to ionized impurities [38], alloy disorder [39], interface roughness [40], LO-phonons and acoustic phonons [41]. The electron temperature was assumed to be 100 K greater than the lattice temperature at all biases. The spatial charge distribution, solutions to the Poisson and Schrödinger equations and scattering rates were then computed iteratively until a self-consistent result was found. Finally, the resulting eigenstates and subband populations were used to compute the intersubband optical gain of the device [42].

Fig. 4 shows the maximum simulated gain of the active region over a range of applied biases. It can be seen that two peaks in the simulated gain occur at biases of 12.6 and 12.9 kV/cm, corresponding to voltage drops of 12.6 and 12.9 V, respectively, across the 10 μ m active region stack. These features arise from changes in the overlap between the wavefunctions for the upper and lower laser subbands. The simulated voltages agree well with the experimental values, with the shortfall being attributed to the effects of contact impedance.

Having obtained the power–current relationship for the QCL, it is possible to predict the dynamic detector behavior for an arbitrary QCL current trace. We have applied the derived transfer-function to the measured current pulses in order to simulate the time-dependent detector signals, and compared the results with the measured traces. For simulations, the transfer function obtained from the NbN detector measurements was used. Fig. 5 shows the measured and simulated dynamic detector signals for two different bias

voltages. All signals are normalized to the global maximum of the modeled traces at all bias voltages. In this way, the amplitudes of measured and simulated pulses are directly comparable for different bias voltages. In general, a very good agreement between simulated and measured pulses has been observed with respect to amplitude, shape and transient features. Nevertheless, differences appear near the rising edge of the pulses: the first peak of the modeled curves is smaller than that of the measured curves for nearly all bias points (see Fig. 5a-I and Fig. 5b-I). Also, for some applied biases, an additional pulse appears before the main pulse in the experimental data, which is never replicated in the modeled response (see Fig. 5b-II). This pre-pulse correlates directly to the transient peak in the center of the rising edge of the current curves (see Fig. 2a-III, for example). As previously mentioned, the reason for those two effects can be found in the limited bandwidth of the current probe. For fast current spikes, the probe is not able to follow the real signal and measures lower values. In comparison to the measured detector pulses, this leads to smaller signals in the simulation or even to no signal if the measured current is below the threshold level. Such issues could be resolved through use of a faster current probe. Another important parameter for characterization of laser performance is the emitted pulse energy E_p . The dependence of E_p on the QCL bias voltage setting U_b (i.e., the nominal output of the pulse generator) was studied by integration of the time-dependent detector signal over the duration of the excitation pulse for each value of U_b . This evaluation was carried out for both the NbN and the YBCO detectors, as well as for the simulated detector pulses based on the previously described NbN transfer function. For comparison the three different curves are shown in Fig. 6. All results are normalized to the maximum of the model curve. There is a good agreement between the curves. For low bias voltages ($U_b < 12.2$ V) the entire QCL current pulse is below threshold, and therefore no radiation is detected. For voltages $U_b > 14.0$ V a strong drop of the pulse energy can be observed because in this case the plateau of the current pulse exceeds the cut-off value, and lasing only occurs during the transient parts of the pulse. In contrast, high pulse energies are obtained for operating points where the current-pulse plateau reaches values that are correlated with high power emission according to the transfer function. For the analyzed QCL, this was the case for $U_b = 12.8$ – 14.0 V with a maximum ranging from 13.7 – 13.9 V. A slight discrepancy between the measured results and the modeled curve is observed in the range $U_b = 14.6$ – 16.2 V (indicated by the dashed ellipse in Fig. 6). This can be explained by the appearance of the pre-pulse for high voltages, as described above. The pre-pulse becomes obvious for voltages $U_b > 14.0$ V because at these bias points the spike which occurs at the center of the rising edge of the current traces exceeds the threshold level. The amplitude of the detected pre-pulse increases until a bias voltage of $U_b = 15.4$ V. Simultaneously, the amplitude of the main pulse decreases because the plateau values of the corresponding current pulses reach the cut-off level. Therefore, the pre-pulse contributes a significant amount of the total pulse energy.

Since this effect is not taken into account by the simulation due to the inaccurate acquisition of the amplitude of the current spike, the corresponding $E_p(U_b)$ curve is below the measured curves in this range. For even higher bias voltages the mentioned current-spike also approaches the cut-off level and the total pulse energy converges to the zero-level for bias voltages $U_b > 16.4$ V, comparable to the simulated curve.

B. Measurement and analysis of QCL emission dependent on pulse length

The dependence of the detector signal on the duration of the excitation pulse Δt was analyzed. The pulse length was tuned from 10 – 500 ns, whilst the bias voltage was set at a constant level of $U_b = 13.9$ V to achieve maximum radiation pulse energy. The pulse repetition rate, operating temperature and detector parameters were set to the same values as described above. The results reveal that lasing was obtained only for pulse durations greater than 40 ns. For shorter pulses, the QCL current does not exceed the threshold level because of the finite rise-time of the current pulse. In Fig. 7, the measured QCL current pulses are depicted together with the NbN detector signals for different pulse durations. The simulated signals according to the previously acquired transfer function are also shown in Fig. 7b. All simulated curves are in good agreement with measurement. Based on these measurements, the emitted pulse energy was determined for each pulse duration by calculating the integral value of each detector trace recorded. These values are plotted in Fig. 8, for both the NbN and YBCO detectors, as a function of the pulse energy measured using the calibrated Ge bolometer. The graph clearly reveals a linear dependence, which confirms that the time-dependent detector voltage directly represents the instantaneous power emission of the QCL. The vertical offset of the YBCO curve is due to a higher noise level in comparison to the NbN measurement.

IV. CONCLUSIONS

We have used ultra-fast superconducting NbN and YBCO detectors to measure the transient response, in the nanosecond range, of QCLs operating at a frequency of ~ 3.1 THz. Specific features have been identified in the measured detector signals that could be assigned to transient features in the QCL drive current. We have demonstrated that the time-dependent emission can be strongly affected by relatively small variations in the driving pulse. These measurements have enabled the QCL power–current relationship to be determined by correlating the time-dependent QCL current with the corresponding detector signals. Such measurements cannot be realized with standard detectors like Ge or InSb bolometers due to the much larger time constants. This has allowed us to identify the threshold and cut-off current values for the laser with a good agreement between each detector type, and we have shown that nanosecond-scale transient features can contribute significantly to the emitted energy in the laser pulse.

We have also shown that the power transfer function can be used to predict accurately the dynamic response of the QCL to an arbitrary rapidly-changing drive-current. However, for very

short transient drive-current peaks, the resolution was limited by the bandwidth of the inductive current probe. Nevertheless, the corresponding QCL emission was observed in the detector output signal, indicating that the detector bandwidth exceeds that of the current probe. By analysis of the detected pulse energy for different driving pulse durations, we have established the linearity of both the NbN and YBCO detectors, and have demonstrated excellent correlation with the response of a calibrated helium-cooled Ge bolometer. The latter measurements contain contributions from the entire time-varying current pulse. Nevertheless, the real dependence of QCL emission on drive current may be determined by taking instantaneous measurements with the superconducting detectors. In this context we have shown that the power-current relationship obtained shows significant differences from those obtained with a Ge bolometer that responds only to the integral pulse energy.

The described measurement scheme could be readily applied to the study of ultra-fast modulation and mode-locking of THz-QCLs.

REFERENCES

- [1] G. Scalari, C. Walther, M. Fischer, R. Terazzi, H. Beere, D. Ritchie and J. Faist, "THz and sub-THz quantum cascade lasers", *Laser & Photon. Rev.*, vol. 3, pp. 45–66, 2009.
- [2] S. Kumar, "Recent Progress in Terahertz Quantum Cascade Lasers", *IEEE J. Sel. Top. Quantum Electron.*, vol. 17, pp. 38–47, 2011.
- [3] S. Kumar, A. W. M. Lee, "Resonant-Phonon Terahertz Quantum-Cascade Lasers and Video-Rate Terahertz Imaging", *IEEE J. Sel. Top. Quantum Electron.*, vol. 14, pp. 333–344, 2008.
- [4] B. S. Williams, S. Kumar, Q. Hu and J. L. Reno, "High-power terahertz quantum-cascade lasers", *Electron. Lett.*, vol. 42, pp. 89–90, 2006.
- [5] A. Barkan, F. K. Tittel, D. M. Mittleman, R. Dengler, P. H. Siegel, G. Scalari, L. Ajili, J. Faist, H. E. Beere, E. H. Linfield, A. G. Davies and D. A. Ritchie, "Linewidth and tuning characteristics of terahertz quantum cascade lasers", *Opt. Lett.*, vol. 29, pp. 575–577, 2004.
- [6] M. Tonouchi, "Cutting-edge terahertz technology", *Nat. Photonics*, vol. 1, pp. 97–105, 2007.
- [7] P. Dean, N. K. Saat, S. P. Khanna, M. Salih, A. Burnett, J. Cunningham, E. H. Linfield and A. G. Davies, "Dual-frequency imaging using an electrically tunable terahertz quantum cascade laser", *Opt. Express*, vol. 17, pp. 20631–20641, 2009.
- [8] A. W. M. Lee, Q. Qin, S. Kumar, B. S. Williams, Q. Hu and J. L. Reno, "Real-time terahertz imaging over a standoff distance (>25 meters)", *Appl. Phys. Lett.*, vol. 89, pp. 141125–141127, 2006.
- [9] H.-W. Hubers, S. G. Pavlov, H. Richter, A. D. Semenov, L. Mahler, A. Tredicucci, H. E. Beere and D. A. Ritchie, "High-resolution gas phase spectroscopy with a distributed feedback terahertz quantum cascade laser", *Appl. Phys. Lett.*, vol. 89, p. 061115, 2006.
- [10] P. Khosropanah, W. Zhang, J. N. Hovenier, J. R. Gao, T. M. Klapwijk, M. I. Amanti, G. Scalari and J. Faist, "3.4 THz heterodyne receiver using a hot electron bolometer and a distributed feedback quantum cascade laser", *J. Appl. Phys.*, vol. 104, p. 113106, 2008.
- [11] L. Betz, R. T. Boreiko, B. S. Williams, S. Kumar, Q. Hu and J. L. Reno, "Frequency and phase-lock control of a 3 THz quantum cascade laser", *Opt. Lett.*, vol. 30, pp. 1837–1839, 2005.
- [12] M. Ravaro, C. Manquest, C. Sirtori, S. Barbieri, G. Santarelli, K. Blary, J.-F. Lampin, S. P. Khanna and E. H. Linfield, "Phase-locking of a 2.5 THz quantum cascade laser to a frequency comb using a GaAs photomixer", *Opt. Lett.*, vol. 36, pp. 3969–3971, 2011.
- [13] P. Khosropanah, A. Baryshev, W. Zhang, W. Jellem, J. Hovenier, J. Gao, T. Klapwijk, D. Paveliev, B. Williams, S. Kumar, Q. Hu, J. Reno, B. Klein and J. Hesler, "Phase locking of a 2.7 THz quantum cascade laser to a microwave reference", *Opt. Lett.*, vol. 34, pp. 2958–2960, 2009.
- [14] S. Barbieri, M. Ravaro, P. Gellie, G. Santarelli, C. Manquest, C. Sirtori, S. P. Khanna, E. H. Linfield and A. Giles Davies, "Coherent sampling of active mode-locked terahertz quantum cascade lasers and frequency synthesis", *Nat. Photonics*, vol. 5, pp. 306–313, 2011.
- [15] G. Scalari, L. Ajili, J. Faist, H. Beere, E. H. Linfield, D. Ritchie and G. Davies, "Far-infrared ($\lambda=87\ \mu\text{m}$) bound-to-continuum quantum-cascade lasers operating up to 90 K", *Appl. Phys. Lett.*, vol. 82, p. 3165, 2003.
- [16] A. Semenov, O. Cojocari, H.-W. Hübers, Song Fengbin, A. Klushin, A.-S. Müller, "Application of Zero-Bias Quasi-Optical Schottky-Diode Detectors for Monitoring Short-Pulse and Weak Terahertz Radiation", *IEEE Electron. Device Lett.*, vol. 31, pp. 674–676, 2010.
- [17] Virginia Diodes, Inc. [Online]. Available: <http://vadiodes.com/>.
- [18] R. Yuan, M. Wei, Y. Qi-Jun, Z. Wen and S. Sheng-Cai, "Terahertz Direct Detection Characteristics of a Superconducting NbN Bolometer", *Chin. Phys. Lett.*, vol. 28, p. 010702, 2011.
- [19] M. Nahum, Q. Hu, P. L. Richards, S. A. Sachtjen, N. Newman and B. F. Cole, "Fabrication and measurement of high T_c superconducting microbolometers", *IEEE Trans. Magn.*, vol. 27, pp. 3081–3084, Mar 1991.
- [20] P. Gellie, S. Barbieri, J. F. Lampin, P. Filloux, C. Manquest, C. Sirtori, I. Sagnes, S. P. Khanna, E. H. Linfield, A. G. Davies, H. Beere and D. Ritchie, "Injection-locking of terahertz quantum cascade lasers up to 35 GHz using RF amplitude modulation", *Opt. Express*, vol. 18, pp. 20799–20816, 2010.
- [21] H. Luo, S. R. Laframboise, Z. R. Wasilewski, G. C. Aers, H. C. Liu and J. C. Cao, "Terahertz quantum-cascade laser based on a three-well active module", *Appl. Phys. Lett.*, vol. 90, p. 041112, 2007.
- [22] H. Callebaut, S. Kumar, B. S. Williams, Q. Hu and J. L. Reno, "Analysis of transport properties of terahertz quantum cascade lasers", *Appl. Phys. Lett.*, vol. 83, p. 207, 2003.
- [23] Y. Chassagneux, Q. J. Wang, S. P. Khanna, E. Strupiechonski, J. Coudeville, E. H. Linfield, A. G. Davies, F. Capasso, M. A. Belkin and R. Colombelli, "Limiting Factors to the Temperature Performance of THz Quantum Cascade Lasers Based on the Resonant-Phonon Depopulation Scheme", *IEEE Trans. THz Sci. Technol.*, vol. 2, pp. 83–92, Jan. 2012.
- [24] H. Richter, A. D. Semenov, S. G. Pavlov, L. Mahler, A. Tredicucci, H. E. Beere, D. A. Ritchie, K. S. Il'in, M. Siegel and H.-W. Hubers, "Terahertz heterodyne receiver with quantum cascade laser and hot electron bolometer mixer in a pulse tube cooler", *Appl. Phys. Lett.*, vol. 93, p. 141108, 2008.
- [25] K. Ilin, R. Schneider, D. Gerthsen, A. Engel, H. Bartolf, A. Schilling, A. Semenov, H.-W. Huebers, B. Freitag and M. Siegel, "Ultra-thin NbN films on Si: Crystalline and superconducting properties", *J. Phys.: Conf. Ser.* 97, p. 012045, 2008.
- [26] P. Probst, A. Scheuring, M. Hofferr, D. Rall, S. Wunsch, K. Il'in, M. Siegel, A. Semenov, A. Pohl, H.-W. Hübers, V. Judin, A.-S. Müller, A. Hoehl, R. Müller and G. Ulm, "YBa₂Cu₃O_{7- δ} quasioptical detectors for fast time-domain analysis of terahertz synchrotron radiation", *Appl. Phys. Lett.*, vol. 98, p. 043504, 2011.
- [27] P. Probst et al., "High-speed Y-Ba-Cu-O direct detection system for monitoring picosecond THz pulses", *Proceedings of the 23rd Int. Symposium on Space Terahertz Technology (ISSTT)*, submitted for publication.
- [28] K. S. Il'in, M. Lindgren, M. Currie, A. D. Semenov, G. N. Gol'tsman, R. Sobolewski, S. I. Cherednichenko and E. M. Gershenzon, "Picosecond hot-electron energy relaxation in NbN superconducting photodetectors", *Appl. Phys. Lett.*, vol. 76, p. 2752, 2000.
- [29] A. D. Semenov, G. N. Gol'tsman and R. Sobolewski, "Hot-electron effect in superconductors and its applications for radiation sensors", *Supercond. Sci. Technol.*, vol. 15, p.1, 2002.
- [30] M. Lindgren, M. Currie, C. Williams, T. Y. Hsiang, P. M. Fauchet, R. Sobolewski, S. H. Moffat, R. A. Hughes, J. S. Preston and F. A. Hegmann, "Intrinsic picosecond response times of Y-Ba-Cu-O superconducting photodetectors", *Appl. Phys. Lett.*, vol. 74, p. 853, 1999.
- [31] M. Lindgren, M. Currie, C. A. Williams, T. Y. Hsiang, P. M. Fauchet, R. Sobolewski, S. H. Moffat, R. A. Hughes, J. S. Preston and F. A. Hegmann, "Ultrafast photoresponse in microbridges and pulse propagation in transmission lines made from high- T_c superconducting Y-Ba-Cu-O thin films", *IEEE J. Sel. Top. Quantum Electron.*, vol. 2, pp. 668–678, Sep. 1996.
- [32] QMC Instruments Ltd. [Online]. Available: <http://www.terahertz.co.uk/>.
- [33] A. D. Semenov, R. S. Nebosis, Yu. P. Gousev, M. A. Heusinger and K. F. Renk, "Analysis of the nonequilibrium photoresponse of

- superconducting films to pulsed radiation by use of a two-temperature model”, *Phys. Rev. B*, vol. 52, pp. 581–590, 1995.
- [34] A. D. Semenov, H.-W. Hubers, K. S. Il'in, M. Siegel, V. Judin and A.-S. Muller, “Monitoring coherent THz-synchrotron radiation with superconducting NbN hot-electron detector”, 34th International Conference on Infrared, Millimeter, and Terahertz Waves, vol. 1, pp. 21–25, 2009.
- [35] D. Garcia, “Robust smoothing of gridded data in one and higher dimensions with missing values”, *Computational Statistics & Data Analysis*, vol. 54, pp. 1167–1178, 2010.
- [36] A. Valavanis, T. V. Dinh, L. J. M. Lever, Z. Ikonic and R. W. Kelsall, “Material configurations for n-type silicon-based terahertz quantum cascade lasers”, *Phys. Rev. B*, vol. 83, p. 195321, 2011.
- [37] J. D. Cooper, A. Valavanis, Z. Ikonic, P. Harrison and J. E. Cunningham, “Finite difference method for solving the Schrödinger equation with band nonparabolicity in mid-infrared quantum cascade lasers”, *J. Appl. Phys.*, vol. 108, p. 113109, 2010.
- [38] T. Unuma, M. Yoshita, T. Noda, H. Sakaki and H. Akiyama, “Intersubband absorption linewidth in GaAs quantum wells due to scattering by interface roughness, phonons, alloy disorder, and impurities”, *J. Appl. Phys.*, vol. 93, p. 1586, 2003.
- [39] G. Bastard and J. Schulman, “Wave Mechanics Applied to Semiconductor Heterostructures”, *Phys. Today*, vol. 45, p. 103, 1992.
- [40] A. Valavanis, Z. Ikonic and R. W. Kelsall, “Intersubband carrier scattering in n- and p-SiSiGe quantum wells with diffuse interfaces”, *Phys. Rev. B*, vol. 77, pp. 075312-075319, Feb. 2008.
- [41] P. Harrison, “Quantum Wells, Wires and Dots”, 3rd ed. Wiley, Chichester, 2009.
- [42] J. H. Davies, “The Physics of Low-Dimensional Semiconductors: An Introduction”, Cambridge University Press, Cambridge, 1998.

Alexander Scheuring received the Diploma Degree in electrical engineering from the University of Karlsruhe, Germany, in 2007.

In April 2007 he joined the Institute of Micro- and Nanoelectronic systems, University of Karlsruhe (later Karlsruhe Institute of Technology). He works on the design and development of quasi-optical receiver concepts for superconducting THz radiation detectors. From February 2008 to July 2008 he was with the LGEP-Supelec in Paris, France, where he was involved in the development of ultra-wideband high-impedance antennas for semiconducting room-temperature THz bolometers.

Paul Dean received the M.Phys. (Hons.) degree in physics in 2001 and the Ph.D. degree in laser physics in 2005, both from the University of Manchester, Manchester, U.K.

In 2005, he was appointed as a Post-Doctoral Research Associate at the Institute of Microwaves and Photonics, School of Electronic and Electrical Engineering, University of Leeds, Leeds, U.K., and as a University Research Fellow in 2011. His current research interests include terahertz optoelectronics, quantum cascade lasers, and terahertz imaging techniques.

Alex Valavanis was born in Maidstone, U.K., in 1981. He received the M.Eng. (Hons) degree in electronic engineering from the University of York, York, U.K., in 2004, and the Ph.D. degree in electronic and electrical engineering from the University of Leeds, Leeds, U.K., in 2009.

From 2004–5, he was an instrumentation engineer at CCLRC Daresbury Laboratories, Warrington, U.K. He is currently a Research Fellow at the University of Leeds. His research interests include quantum cascade lasers, terahertz sensors, silicon photonics, and computational methods for quantum electronics.

Dr. Valavanis is a member of the Institution of Engineering and Technology (IET).

Axel Stockhausen received the Diploma Degree in physics from the University of Karlsruhe, Germany, in 2007.

In October 2007 he joined the Institute of Micro- and Nanoelectronic systems, University of Karlsruhe (later Karlsruhe Institute of Technology) as a Staff member. He works on the development and optimization of superconducting hot-electron bolometers for the THz frequency range.

Petra Thoma received the Diploma Degree in electrical engineering and information technologies from the Karlsruhe Institute of Technology, Germany, in 2009.

In November 2009 she joined the Institute of Micro- and Nanoelectronic systems, Karlsruhe Institute of Technology. Her main research area is the development of high-temperature YBCO superconducting detectors for ultra-

fast pulse measurements in the THz frequency range. These detectors are used for the characterization of picosecond THz pulses emitted at electron storage rings.

Mohammed Salih received the B.Sc. degree in Electrical Engineering from the University of Mosul, Iraq, in 1993, the M.Sc. degree in Electrical Engineering from the University of Kassel, Germany, in 2002 and the Ph.D. degree in Electronic and Electrical Engineering from the University of Leeds, Leeds, U.K., in 2011.

He works currently as a postdoctoral Research Fellow at the University of Leeds. His research interests include the fabrication and characterization of terahertz quantum cascade lasers.

Suraj P. Khanna received the B.Eng. degree (first class) in electronics and telecommunications engineering from the University of Amravati, Amravati, India, in 2001, and the M.Sc. degree in nanoscale science and technology and the Ph.D. degree in electronic and electrical engineering from the University of Leeds, Leeds, U.K., in 2004 and 2008, respectively.

From 2008–2011, he was a Postdoctoral Research Associate at the University of Leeds. He is currently a Research Fellow at Northwestern University, USA. His current research interests include molecular beam epitaxial growth, MOCVD growth of dilute magnetic semiconductors, semiconductor device fabrication, quantum cascade lasers, and terahertz-frequency optical systems.

Siddhant Chowdhury was born in Kolkata, India, in 1990. He received the B.Eng degree in electronics and nanotechnology from the University of Leeds, Leeds, UK, in 2011.

Following graduation, he worked as a Summer Intern in the Institute of Microwaves and Photonics (IMP) at the University of Leeds and is currently pursuing his PhD in the same institute. His research interests include terahertz quantum cascade lasers and their applications.

Jonathan D. Cooper was born in Aldershot, U.K. in 1988. He received the B.Eng. (hons.) degree in electronic engineering from the University of Leeds, U.K. in 2009.

Since 2009 he has been studying towards the Ph.D. degree in electronic engineering within the Institute of Microwaves and Photonics at the University of Leeds. His research interests include quantum electronics, computational physics and optoelectronic devices.

Andrew Grier was born in Belfast, Northern Ireland. He received the B.Sc. (Hons.) degree in physics from the University of St. Andrews, St. Andrews, U.K. in 2009 and the M.Sc. degree in nanotechnology and advanced electronic devices from the University of Leeds, Leeds, U.K. in 2010.

Since 2011, he has been pursuing the Ph.D. degree in electronic and electrical engineering at the Institute of Microwaves and Photonics at the University of Leeds. His research interests include numerical simulations of bandstructure and charge transport phenomena in quantum cascade lasers and nitride based intersubband devices.

Stefan Wuensch received the Dipl.-Ing. and Dr.-Ing. degrees in electrical engineering from the University of Karlsruhe, Germany, in 1998 and 2005, respectively.

In November 1998, he joined the Institut fuer Elektrotechnische Grundlagen der Informatik, University of Karlsruhe. In September 2002, he joined the Institut fuer Mikro- und Nanoelektronische Systeme, University of Karlsruhe. His main research interest are passive microwave devices for detector applications and cryogenic microwave amplifiers for detector readout systems.

Konstantin Il'in was born in Moscow, Russia, on March 24, 1968. He received the Ph.D. degree in solid-state physics from Moscow State Pedagogical University (MSPU), Moscow, Russia, in 1998.

From 1997 to 1998, he was a Visiting Scientist with the Electrical and Computer Engineering Department, University of Massachusetts at Amherst, and with the Electrical Engineering Department, University of Rochester, Rochester, NY. From January 1998 to June 1999, he was an Assistant Professor with the Physics Department, MSPU. From 1999 to 2003, he was a Scientific Researcher with the Institute of Thin Films and Interfaces, Research Center Juelich, Juelich, Germany. In June 2003, he joined the Institute of Micro- and Nano-electronic Systems, University of Karlsruhe, Karlsruhe, Germany, where he currently develops technology of ultrathin films of conventional superconductors for receivers of electromagnetic radiation. His research interests include fabrication and study of normal state and

superconducting properties of submicrometer- and nanometer-sized structures from ultrathin films of disordered superconductors.

Edmund H. Linfield received the M.A degree in physics and the Ph.D. degree in semiconductor physics from the University of Cambridge, Cambridge, U.K. in 1986 and 1991 respectively.

He continued his research as a Post-Doctoral Researcher Associate with the Cavendish Laboratory, University of Cambridge, until 1997, when he was appointed as an Assistant Director of Research. He also became a Fellow of Gonville and Caius College, Cambridge. In 2004, he moved to the University of Leeds, Leeds, U.K., to take up the Chair of Terahertz Electronics. He is currently also Director of Research in the School of Electronic and Electrical Engineering, and was awarded the "Dream Fellowship" (2011) from the Engineering and Physical Sciences Research Council. His research interests include semiconductor growth and device fabrication, terahertz-frequency optics and electronics, and nanotechnology.

Giles Davies received the first class B.Sc. (Hons.) degree in chemical physics from the University of Bristol, Bristol, U.K., in 1987 and the Ph.D. degree in semiconductor physics from the Cavendish Laboratory, University of Cambridge, Cambridge, U.K., in 1991.

After spending three years as an Australian Research Council Postdoctoral Research Fellow with the University of New South Wales, Sydney, Australia, he returned to the University of Cambridge in 1995 as a Royal Society University Research Fellow. In 2002 he moved to the University of Leeds, Leeds, U.K., to take up the Chair of Electronic and Photonic Engineering, where he is currently also Deputy Head of the School of Electronic and Electrical Engineering, and Pro-Dean for Research and Innovation in the Faculty of Engineering. His research interests include semiconductor nanostructures, terahertz-frequency optics and electronics, and bionanotechnology.

Prof. Davies is a Fellow of the Institute of Physics. He is a member of the editorial board of the IEEE Transactions on Terahertz Science and Technology, and he received the Royal Society Wolfson Foundation Research Merit Award in 2011.

Michael Siegel received the Diploma Degree in physics and the Ph.D. degree in solid state physics from the Moscow State University, Moscow, Russia, in 1978 and 1981, respectively.

In 1981, he joined the University of Jena where he held positions as Staff Member and later as Group Leader in the Superconductive Electronic Sensor Department. His research was oriented on non-linear superconductor-semiconductor devices for electronic applications. In 1987, he initiated research at the University of Jena in thin-film high temperature superconductivity (HTS) for Josephson junction devices, mainly for SQUID. In 1991, he left to join the Institute for Thin Film and Ion Technology at Research Center Juelich. There he worked on development and application of HTS Josephson junctions, SQUID, microwave arrays and mixers, and high-speed digital circuits based on rapid-single-flux-quantum logic. In 2002, he received a Full Professor position at University of Karlsruhe, Germany, where he is now the Director of the Institute of Micro- and Nanoelectronic Systems. His research includes transport phenomena in superconducting, quantum and spin dependent tunneling devices. He has authored over 200 technical papers.

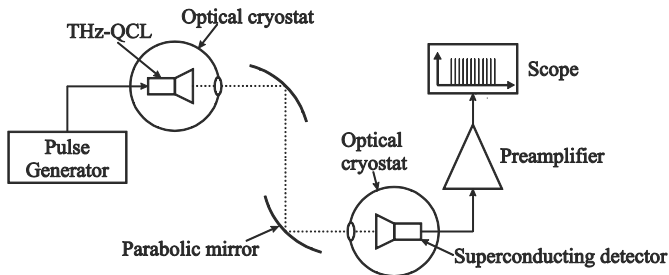


Fig. 1. Schematic diagram showing the experimental apparatus.

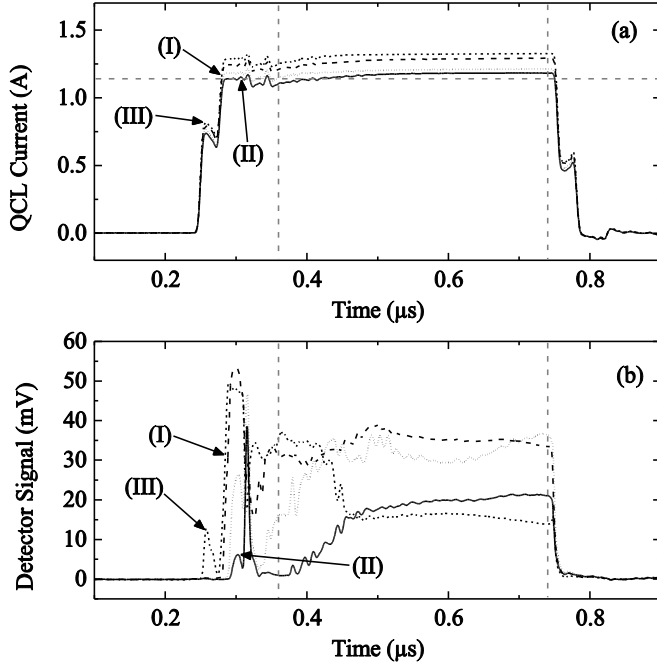


Fig. 2. (a) Measured QCL current as a function of time for different bias voltages: $U_b=12.6$ V (solid), $U_b=13.0$ V (dots), $U_b=13.7$ V (dashes) and $U_b=14.1$ V (short dashes). The dashed horizontal line indicates the threshold current of the laser, the dashed vertical lines mark the temporal-range used to obtain the QCL power transfer-function. (b) Measured NbN detector signal over time for the corresponding bias voltages. Special transient features are indicated by (I)–(III) (see text for details).

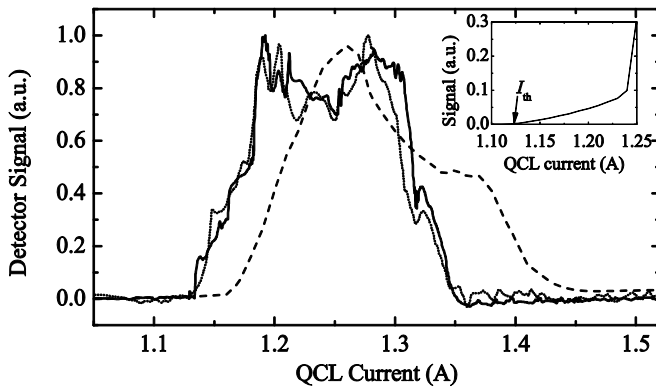


Fig. 3. QCL power transfer function (detector signal vs. QCL current) derived from NbN (solid) and YBCO (dotted) detector measurements. For comparison, the transfer function obtained from time-averaged Ge-bolometer measurements (dashed) is shown. The inset shows the Ge bolometer signal near the threshold current.

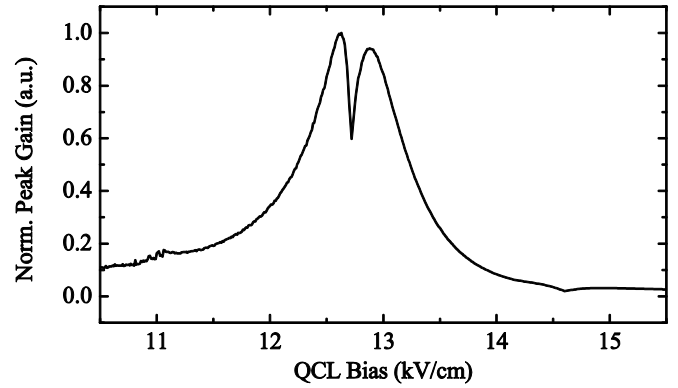


Fig. 4. Simulated gain of the QCL as a function of the applied bias. Comparable to the measurements of the superconducting detectors, the simulated characteristic shows a double-peak which is caused by the overlap of the wavefunctions of the laser subbands.

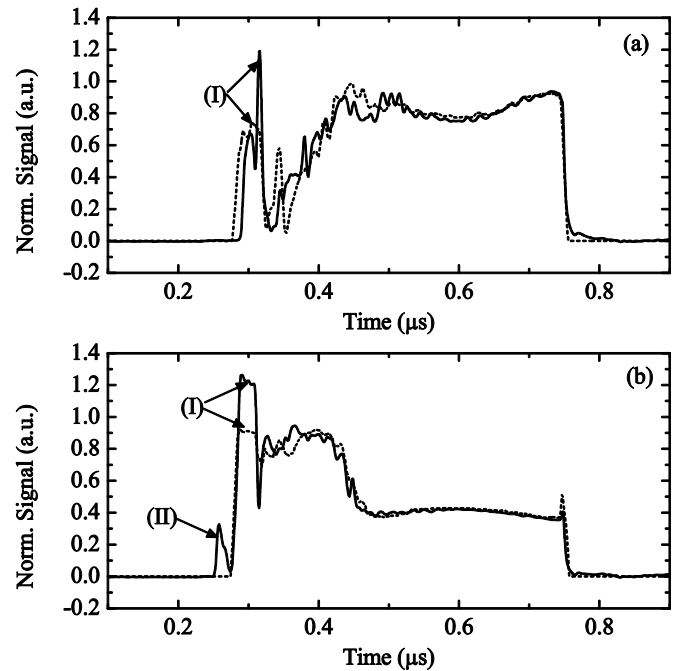


Fig. 5. Measured (solid) and modeled (dashed) NbN detector signals as a function of time for (a) $U_b=13.0$ V and (b) $U_b=14.1$ V. (I)-(II) mark specific discrepancies between measurement and simulation (see text).

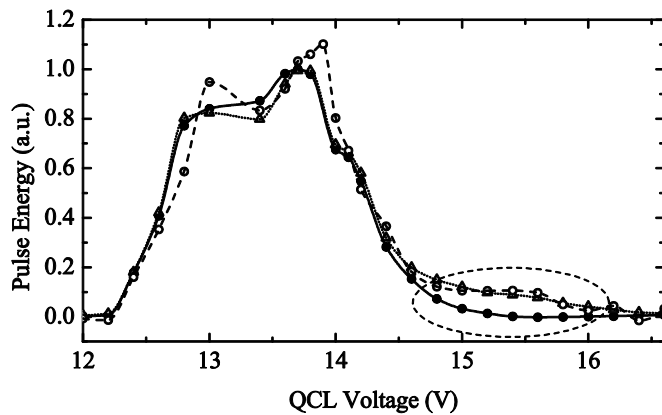


Fig. 6. Radiation energy E_p dependence on QCL bias voltage setting U_b for the NbN transfer-function model (\bullet), NbN (\triangle) and YBCO (\circ) detector measurements. Lines are a guide to the eye. The dashed ellipse marks the part where the measured traces differ from the simulated one due to the pre-pulse (see text).

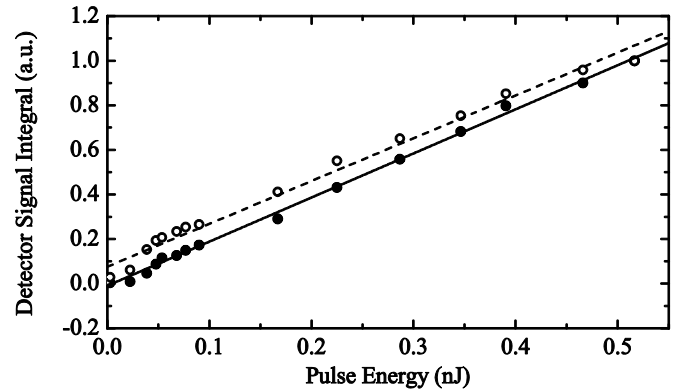


Fig. 8. Integrated detector signal (symbols) as a function of pulse energy for the NbN (\bullet) and YBCO (\circ) detectors. The pulse energy values were obtained from Ge bolometer measurements. The lines are linear fits.

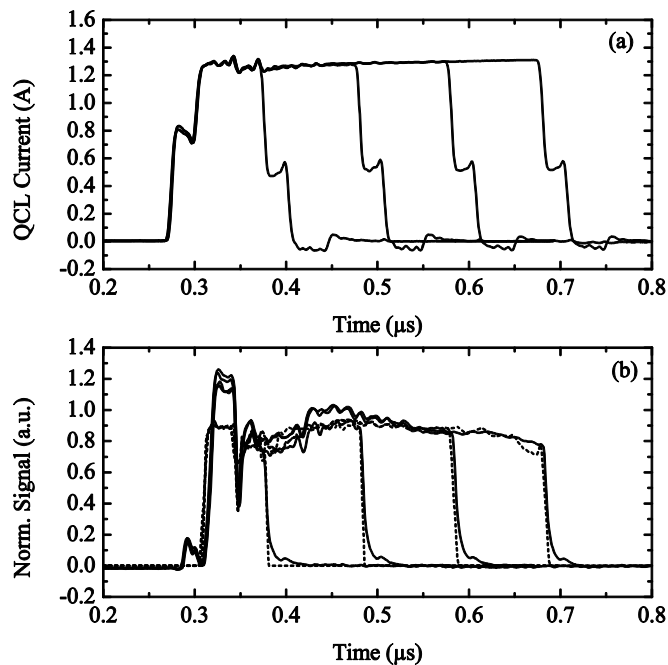


Fig. 7. (a) Measured QCL current over time for different pulse durations: $\Delta t=100$ ns, 200 ns, 300 ns and 400 ns. (b) Measured (solid) and modeled (dashed) NbN detector signals for the corresponding pulses.

TABLE I
GEOMETRICAL AND ELECTRICAL DETECTOR PARAMETERS

Type	NbN	YBCO
Width (μm)	1.0	4.5
Length (μm)	0.5	2.0
Thickness (nm)	5	45
Bias voltage (mV)	6	100
Bias current (mA)	0.05	9.7
Operation temperature T_{op} (K)	11.0	70
Critical temperature T_c (K)	12.2	85